

## Strange attractor of the modulated Stokes wave: A universal form

Hie Tae Moon

*Physics Department, Korea Advanced Institute of Science and Technology, Daeduk Science-town 305-701, Korea*

(Received 22 September 1992)

This Rapid Communication argues that the strange attractor recently found in the context of the modulated Stokes wave [H. T. Moon, *Phys. Fluids A* **3**, 2709 (1991)] is a universal form and indeed the asymmetric counterpart of the Lorenz attractor. Furthermore, this form appears to reveal another class of universality in that it follows the evolution pattern set by the tent map. This is in marked contrast to the Rössler attractor, which follows the universal sequence of the logistic map.

PACS number(s): 05.45.+b, 47.20.Ky, 47.27.Cn

Since the discovery of the chaotic attractor by Lorenz [1], chaos has become an important concept in nearly all branches of natural sciences. Incidentally, the Lorenz attractor itself has been one of the subjects of the most intensive studies. One of the natural questions that followed the Lorenz attractor was on its symmetry, essential to the global structure. Rössler [2], also motivated by the question, was able to extract an asymmetric structure from his proposed equations. This structure, called the Rössler attractor, however, has a different folding mechanism. Since then these two attractors have become two principal paradigms for chaotic attractors. They are in fact prototypes of two broad categories of chaotic attractors [3]. In one type, folding is accomplished by splitting, or homoclinic crossings, while in the other category the folding is accomplished by a continuous bending in phase space. Notably, they are both reducible into a one-dimensional map with a remarkable simplicity.

Whether the Lorenz attractor has its asymmetric counterpart still remains open, but such a structure, if it exists, would be essential to the understanding of the possible basic forms of the chaotic attractors. The purpose of this Rapid Communication is to argue that the strange attractor recently found in the context [4] of the modulated Stokes wave (abbreviated to SAMS) is indeed the asymmetric counterpart of the Lorenz attractor, and also a universal form. Furthermore, this form appears to exhibit another kind of universality in that it follows the evolution patterns of the algebraically defined tent map. This is in marked contrast with the Rössler attractor which follows the universal evolution schemes of the smooth logistic map [3]. Despite the difference in the underlying folding mechanisms, there appears a profound parallelism existing between SAMS and the Rössler attractor. This point is made clear throughout the study by comparing the characteristic features of SAMS with those of the Rössler attractor.

Briefly, I would like to introduce here the origin of SAMS. The Stokes wave is important in many disciplines of physics, and the modulational instability associated with it has been a long-standing problem [5]. It needs, however, to be studied through the partial differential equation known as the Ginzburg-Landau (GL) equation [6]. The existence of a strange attractor near the Stokes wave was known for some time [7], but the concrete ap-

pearance of its topological structure has been known only recently [4]. The detailed geometric information of the phase portraits is now available through an analysis of a much simpler reduced phase space. The attractor obtained in the new space is not meant to be identical to that in the original space, though the new representation may retain the same topological properties if it is not too complicated. The Stokes wave, under given conditions, evolves into one of three definite wave patterns, whose orbits, in a reduced space, can be found globally connected by a double homoclinic orbit [4]. The dynamics soon become unstable and the resulting spatial patterns underlined by temporal chaos are then attributed to the homoclinic orbit. It is this strange attractor which we all SAMS here.

We start by presenting the one-dimensional (1D) map of SAMS in Fig. 1(a). The 1D map of the Rössler attractor is also presented in Fig. 1(b) for comparison. The two attractors are obtained from the following dynamical systems, known, respectively, as the Ginzburg-Landau and the Rössler equations:

$$\psi_t = \psi + (1 + ic_d)\psi_{xx} - (1 + ic_n)|\psi|^2\psi, \quad (1)$$

$$\dot{x} = -y - z, \quad \dot{y} = x + \alpha y, \quad \dot{z} = \beta + xz - \sigma z, \quad (2)$$

where the coefficients are set  $c_d = 5, c_n = -4$  for Eq. (1) and  $\alpha = 0.2, \beta = 0.2, \sigma = 4.55$  for Eq. (2). Equation (1) possesses an equilibrium solution known as the Stokes wave  $\psi_s(t) = e^{-ic_n t}$ , which is modulated initially by the sideband waves as  $\psi(x, 0) = \psi_s(0) + 0.05e^{(iqx)} + 0.05e^{(-iqx)}$ . The sideband wave number  $q$  is the control parameter. Figure 1(a) was obtained for  $q = 0.924$  by plotting  $Q_{n+1}$ , the  $(n+1)$ th maximum of the amplitude of the modulating mode  $|a_q(t)|$ , as a function of  $Q_n$ , the  $n$ th maximum of  $|a_q(t)|$ . The 1D map of the Rössler attractor of Fig. 1(b) was obtained by plotting  $R_{n+1}$ , the  $(n+1)$ th maximum of the variable  $x(t)$ , as a function of  $R_n$ , the  $n$ th maximum of  $x(t)$ .

The two maps look globally similar except the shapes of the maxima: the first map has a sharp peak, whereas the second map has a smooth maximum. In the first map, the slope is everywhere greater than 1 in magnitude except at the peak where the sign changes from positive to negative. In the second, the magnitude of the slope is smaller than 1 near the maximum. With the double

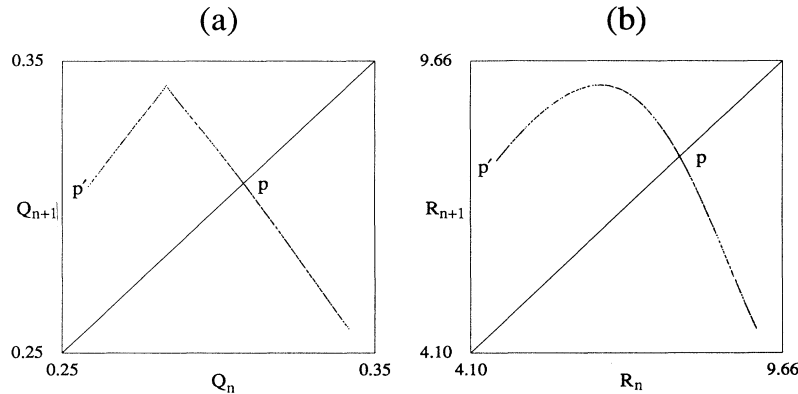


FIG. 1. The one-dimensional maps obtained from the strange attractors. (a) SAMS, (b) the Rössler attractor.  $p$  denotes the unstable fixed point and  $p'$  denotes its antecedent. Reinjection to  $p$  is possible through  $p'$ . They are both asymmetric, but notice the difference in their shapes of the maxima.

homoclinic orbit being the source for chaos, the sharp peak of the first map, like the Lorenz map, is related to the folding mechanism of homoclinic crossings. On the other hand, the smooth maximum of the second map is, as is well known [3], the manifestation of the folding structure of continuous bending. The two maps displayed are therefore exhibiting the difference in their own folding mechanisms.

Figure 2 depicts how SAMS evolves within the chaotic regime, starting from the fixed point denoted by  $a$ . We note that state  $a$  is actually representative for a two-frequency motion; one frequency in the amplitude and the other in the phase. State  $a$  becomes unstable to the attracting set that looks like two points (state  $b$ ) in the resolution of the figure. For values of  $q$  decreasing, it is found that state  $b$  loses its stability to a state having four bands (state  $c$ ), then to a state having two bigger bands (states  $d$  and  $e$ ), and finally to a state with one big band (states  $f$  and  $g$ ). We observe that the final global form of the attractor, i.e., the structure of state  $f$  or  $g$ , remains robust

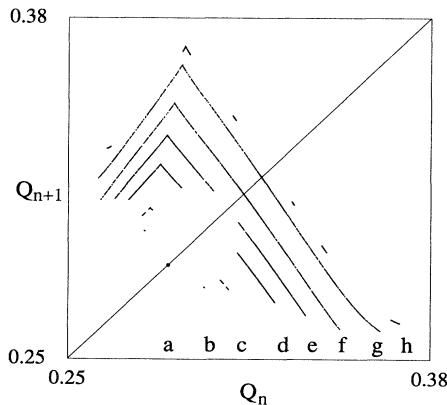


FIG. 2. The evolution of SAMS within the chaotic regime, starting from the fixed point state denoted by  $a$ ;  $a$  ( $q=0.985$ ),  $b$  ( $q=0.980$ ),  $c$  ( $q=0.970$ ),  $d$  ( $q=0.950$ ),  $e$  ( $q=0.936$ ),  $f$  ( $q=0.920$ ),  $g$  ( $q=0.900$ ),  $h$  ( $q=0.890$ ). The final structure before getting out of the chaotic regime, i.e., state  $f$  or  $g$ , is seen ultimately asymmetric. Notice that, since state  $a$  represents a  $T^2$  torus, the evolution patterns also illuminate the manner in which a  $T^2$  torus loses its stability.

until it ceases to be chaotic (see  $h$ ). It is to be noticed that this final structure, unlike the Lorenz attractor, is ultimately asymmetric. Later, we shall compare the evolution patterns shown here with the patterns of the algebraically defined tent map. State  $a$  being  $T^2$  torus, we also note that the bifurcation patterns displayed in Fig. 2 illuminate the manner in which a  $T^2$  torus loses its stability [8].

As found above, the final structure of SAMS is asymmetric and in this paper we are concerned with the dynamic properties of this final structure. It has been seen in Fig. 1 that both SAMS and the Rössler attractor, associated with their asymmetry, have an unstable fixed point and its antecedent, denoted, respectively, by  $p$  and  $p'$ . Thus, the fixed point  $p$ , although unstable, does not disappear, but is revisited through  $p'$ . This reinjection behavior was actually pointed out by Rössler [2] for his system. It is implied by the maps that reinjection in each system takes place with a definite probability. These asymmetric attractors may then be viewed as composed of two *metastable* attractors; one being a chaotic attractor and the other being a periodic attractor. The study of the dynamics then comprises three parts; the chaotic phase, the laminar phase, and the statistics of reinjection.

As for the properties of the chaotic motion alone, we may look at state  $e$  shown in Fig. 2, which does not contain the unstable fixed point  $p$  as part of the attractor. In this case, the attractor consists of two disjoint segments. We refer here to the upper segment of the larger amplitude as the fundamental and the lower segment of the smaller amplitude as the subharmonic. Since every other iteration will bring the iteration back into the same segment, it appears necessary to look at the second return map  $Q_{n+2}=F^2(Q_n)=F(F(Q_n))$  as well. The result is shown in Fig. 3, where the first return map  $F$ , drawn in a faint line, is also inserted for comparison. Figure 3(b) displays the corresponding situation of the Rössler attractor at  $\sigma=4.55$ . We observe that the chaotic behavior of the fundamental, and the chaotic behavior of the subharmonic, are, respectively, described by the familiar Lorenz-type map. The basic structure constituting the chaotic dynamics of SAMS is therefore found to be a combination of two Lorenz-type maps, one for the funda-

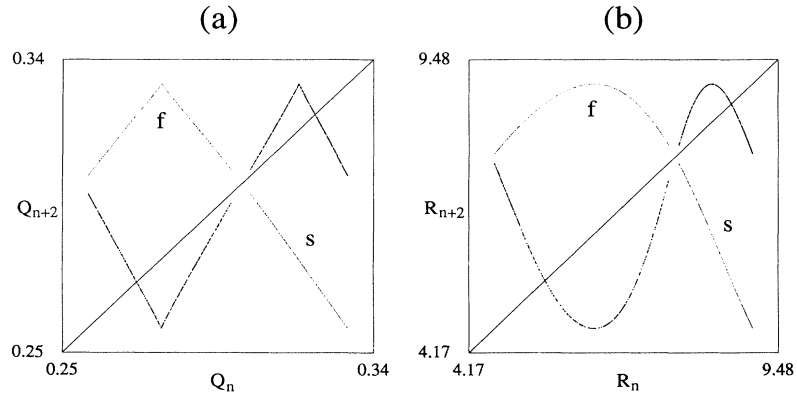


FIG. 3. The second return map,  $Q_{n+2} = F^2(Q_n)$ . (a) SAMS when  $q = 0.932$ , (b) the Rössler attractor when  $\sigma = 4.47$ . The first return map  $Q_{n+1} = F(Q_n)$ , drawn in a faint line, is also inserted for comparison.  $f$  denotes the fundamental and  $s$  denotes the subharmonic. The chaotic behavior of  $f$ , or  $s$ , is described in (a) by the Lorenz type map, while in (b) the full quadratic map.

mental and the other for the subharmonic. On the other hand, the fundamental and the subharmonic, constituting the Rössler attractor, are, respectively, described by the full symmetric quadratic map.

The statistical aspects of the reinjection process of SAMS can be seen clearly by comparing the second return maps obtained, respectively, when the attractor contains, or does not contain, the fixed point  $p$  in it. The result is shown in Fig. 4. The outer bigger map is the one obtained from the state shown in Fig. 1(a) and the inner smaller part is the one obtained from the state shown in Fig. 3(a). For clarity, only the right-hand side from the fixed point  $p$  is plotted. It shows that if, while wandering during a chaotic phase, the trajectory crosses the line denoted by  $e$ , i.e.,  $Q_{n+2} > e$ , the following iterations will bring the trajectory back into the neighborhood of  $p$ . We notice that this picture is identical with the one considered by Yorke and Yorke [9] in their investigation of the transient chaos in the Lorenz system. The differences are twofold. First, Yorke and Yorke considered the first return map, whereas here we considered the second return map. Second, in the transient chaos of the Lorenz system, the fixed point is stable, while here the fixed point is unstable. We note that Yorke and Yorke found numerically that the statistical distribution of the length of the transient chaos was exponential.

Phenomenologically reinjection to  $p$  implies relaminarization and we next compare the phenomenology expressed by SAMS and by the Rössler attractor. In Fig. 5, we plotted the time evolution of  $|a_q(t)|$  of SAMS and the time evolution of  $x(t)$  of the Rössler attractor, in which  $C$  denotes the chaotic phase and  $L$  denotes the laminar phase. The difference between the chaotic phases of the two systems is highly visible. We note first the wild behavior of the periods of the chaotic oscillations of SAMS. Obviously this unpredictability of the periods is the manifestation of the existence of the homoclinic saddle point, the orbit spending varying periods of time depending on the proximity to the saddle point. No such behavior is observed in the Rössler attractor. Given the parabolic form of the one-dimensional map, the chaotic phase of

the Rössler attractor is characterized by period doublings.

The universality of the Rössler attractor is well known in that it follows the universal bifurcation sequence of the logistic map [3]; hence we may look for the analog to SAMS:

$$T_\lambda(x) = \lambda(1 - 2|x - 1/2|) . \tag{3}$$

The above map is the tent map algebraically defined on  $0 \leq x \leq 1$  for  $0 \leq \lambda \leq 1$ . Here  $\lambda$ , a nonlinearity measure, is the control parameter. Figure 6 shows the bifurcation sequence of the tent map starting from the fixed point denoted by  $a$ , which becomes unstable for  $\lambda > 1/2$ . The unstable fixed point is not in the attractor until  $\lambda$  reaches the value  $\lambda = 1/\sqrt{2}$ , where the fixed point, together with its antecedent, becomes part of the attractor (state  $f$ ). Upon comparing the bifurcation patterns with those of SAMS in Fig. 2, we find that the two evolution patterns are identical. This shows that SAMS actually followed in the predetermined path as set by the tent map. We note

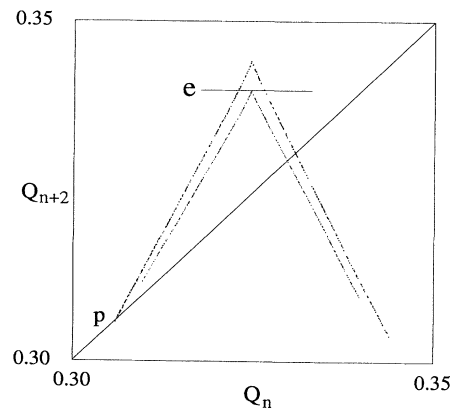


FIG. 4. Statistical aspects of reinjection process. The outer map is the second return map of the subharmonic obtained from the state shown in Fig. 1(a) and the inner map is the one from the state shown in Fig. 3(a). It shows that if, while wandering during a chaotic burst, the iteration crosses the line denoted by  $e$ , i.e.,  $Q_{n+2} > e$ , the following iteration will be brought back into the neighborhood of  $p$ , where a laminar phase starts again.

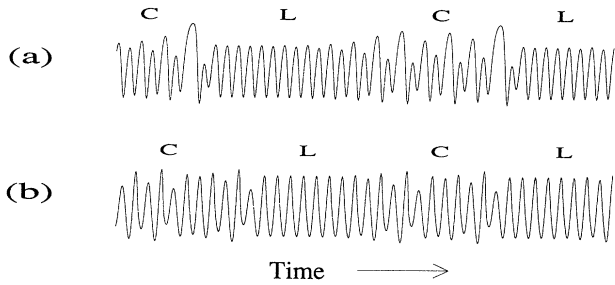


FIG. 5 Intermittent phenomena exhibited (a) by SAMS, and (b) by the Rössler attractor. *C* denotes the chaotic phase and *L* denotes the laminar phase. The difference in the periods of the orbit is visible. In (a), a wild behavior of the periods of the orbit is seen as characteristic, while in (b) the chaotic phase is characterized by period doublings.

that the structure of the tent map at  $\lambda = 1/\sqrt{2}$  corresponds to the final asymmetric form of SAMS. Therefore the tent map is representative of SAMS for a  $\lambda$  in the range of  $1/2 < \lambda \leq 1/\sqrt{2}$ . We point out here that the Lorenz attractor was actually modeled by Lorenz [1] by the tent map with  $\lambda = 1$  at which the map becomes fully symmetric.

The Lyapunov exponent for the tent map, as a function of the nonlinearity  $\lambda$ , is found to be  $L = \ln 2\lambda$ . This infers that the Lyapunov exponent for SAMS grows logarithmically and bounded as  $0 < L \leq \ln \sqrt{2}$ . State *b* of Fig. 2, characterized by two points, is thus chaotic even though in the resolution of the figure it looks like there is a period-two attractor. In addition, since the algebraically defined explicit map makes it amenable to detailed numerical studies, we may model the statistics of reinjection process utilizing the tent map. Without showing, we merely state that it is easily found that the distributions for the length of chaotic phase and for the length of laminar phase are both exponential.

Finally, we point out that the origin of the difference between SAMS and the Lorenz attractor lies in the type of linear instability of the limit cycle existing in each system. The limit cycles are represented by an unstable fixed point in the reduced one-dimensional map. As shown in Fig. 1(a), the fixed point *p* of SAMS has a slope slightly less than  $-1$ . This, in terms of the Floquet matrix, is the case in which the eigenvalue crosses the unit circle of the complex plane at  $-1$ , corresponding to the so-called subharmonic instability. It is well known, on the other hand, that the Lorenz attractor has a pair of very small

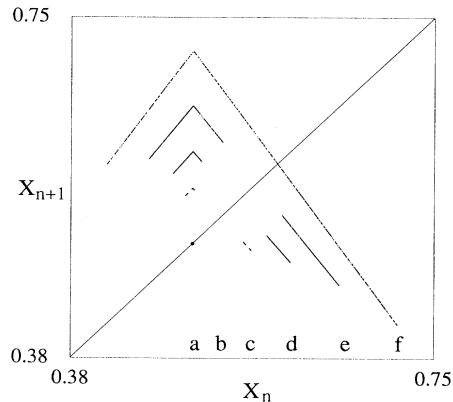


FIG. 6. The bifurcation patterns of the algebraically defined tent map; *a* ( $\lambda = 1/2$ ), *b* ( $\lambda = 0.52$ ), *c* ( $\lambda = 0.56$ ), *d* ( $\lambda = 0.60$ ), *e* ( $\lambda = 0.65$ ), *f* ( $\lambda = 1/\sqrt{2}$ ). The tent map is representative for SAMS for a  $\lambda$  in the range  $1/2 < \lambda \leq 1/\sqrt{2}$ . Note that the tent map symmetric at  $\lambda = 1$  is representative for the Lorenz attractor.

limit cycles of saddle type separated by a symmetric double homoclinic orbit [1]. In its one-dimensional map, either limit cycle reappears as the left bottom part [10] where the slope is slightly greater than  $+1$ , which, in terms of the Floquet multiplier, corresponds to the crossing at  $+1$ . The folding in the Lorenz attractor, in the absence of any subharmonic, is accomplished instead by crossing into the other well, which is, after all, compatible with the symmetry of the Lorenz attractor. In fact, the same Lorenz attractor is also found in the symmetric coupled-disk dynamo system [11]. In short, there exist two types of basic structures in this folding category based on the linear instability of the limit cycle; the symmetric Lorenz type and the symmetric SAMS type.

As a final remark, it has been an exciting idea in recent years that vastly different physical systems may all reduce down to a few universal forms. The Lorenz attractor is a universal form, as is the Rössler attractor. This Rapid Communication asserts that SAMS is another universal form. But this time the significance of the tent map is brought out whose relevance to real complex systems has been unclear.

The author wishes to thank M. J. Kim for the help with the computer graphics. This work was performed under the auspices of the Korea Science and Engineering Foundation and the Center of Thermal and Statistical Physics.

[1] E. N. Lorenz, *J. Atmos. Sci.* **20**, 130 (1963).  
 [2] O. E. Rössler, *Phys. Lett.* **57A**, 397 (1976).  
 [3] See, e.g., J. M. T. Thomason and H. B. Stewart, *Nonlinear Dynamics and Chaos* (Wiley, New York, 1986), Chap. 12.  
 [4] H. T. Moon, *Phys. Fluids A* **3**, 2709 (1991).  
 [5] J. T. Stuart and R. C. Diprima, *Proc. R. Soc. London Ser. A* **362**, 27 (1978).  
 [6] A. C. Newell, *Lect. App. Math.* **15**, 157 (1974).  
 [7] Y. Kuramoto and T. Tsuzuki, *Prog. Theor. Phys.* **54**, 687 (1975); H. T. Moon, P. Huerre, and L.G. Redekopp, *Phys. Rev. Lett.* **49**, 458 (1982); C. R. Doering, J. D. Gibbon, D. D. Holm, and B. Nicolaenko, *Phys. Rev. Lett.* **59**, 2911

(1987); L. Sirovich, J. D. Rodriguez, and B. Knight, *Physica* **43D**, 63 (1990).  
 [8] D. Ruelle and F. Takens, *Commun. Math. Phys.* **20**, 167 (1971): the transition to chaos from a  $T^2$  torus is a well-known scenario from Ruelle and Takens.  
 [9] J. A. Yorke and E. D. Yorke, *J. Stat. Phys.* **21**, 263 (1979).  
 [10] The unstable fixed point in the right-hand side of the maximum of the Lorenz map, whose slope is much less than  $-1$ , is simply a by-product of repeated homoclinic crossings between the two symmetric wells.  
 [11] A. E. Cook and P. H. Roberts, *Proc. Cambridge Philos. Soc.* **68**, 547 (1970).